2011

A cytoplasm-specific activity encoded by the Trithorax-like ATX1 gene

Ivan Ndamukong
University of Nebraska-Lincoln

Hanna Lapko
University of Nebraska-Lincoln, hlapko2@unl.edu

Ronald L. Cerny
University of Nebraska-Lincoln, rcerny1@unl.edu

Zoya Avramova
University of Nebraska-Lincoln, zavramova2@unl.edu

Published online 17 January 2011 *Nucleic Acids Research, 2011, Vol. 39, No. 11* ***4709–4718***
doi:10.1093/nar/gkq1300

A cytoplasm-specific activity encoded by the Trithorax-like ATX1 gene

Ivan Ndamukong[1], Hanna Lapko[1], Ronald L. Cerny[2] and Zoya Avramova[1,*]

[1]School of Biological Sciences and [2]Department of Chemistry, University of Nebraska, Lincoln

Received October 8, 2010; Revised November 8, 2010; Accepted December 4, 2010

ABSTRACT

Eukaryotes produce multiple products from a single gene locus by alternative splicing, translation or promoter usage as mechanisms expanding the complexity of their proteome. Trithorax proteins, including the *Arabidopsis* Trithorax-like protein ATX1, are histone modifiers regulating gene activity. Here, we report that a novel member of the Trithorax family has a role unrelated to chromatin. It is encoded from an internal promoter in the *ATX1* locus as an isoform containing only the SET domain (soloSET). It is located exclusively in the cytoplasm and its substrate is the elongation factor 1A (EF1A). Loss of SET, but not of the histone modifying ATX1-SET activity, affects cytoskeletal actin bundling illustrating that the two isoforms have distinct functions in *Arabidopsis* cells.

INTRODUCTION

The highly conserved (~150 amino acids) SET [Su(var)3-9, E(z), Trithorax] domain is found in chromatin proteins involved in both gene repressing and gene activating complexes. The SET domains have an intrinsic preference for specific histone lysine-residues (1). A methylation sign at a particular histone lysine defines the transcriptional state of the involved gene (2). SET domain-containing proteins of the TRITHORAX family, including ATX1, specifically methylate lysine 4 of histone H3 (H3K4me) (3,4). Loss of ATX1-function has pleiotropic effects in *Arabidopsis* affecting development, organogenesis (5), and ability to respond to biotic (6) and abiotic (7) stresses. ATX1 is not involved in a genome-wide H3K4 methylation but, instead, targets specific genes (8). Increased levels in nucleosomal H3K4me3 marks of ATX1-regulated genes correlates with elevated transcript levels (3,8) defining ATX1 as a histone modifier and as a positive effector of gene expression.

Trithorax proteins carry signature structural domains [FYRN-FYRC (DAST), PHD and SET] plus additional clade-specific domains (9,10). A combinatorial assembly of various peptide domains generates possibilities for diversification and precision of function (11). The best studied SET domain proteins function in the nucleus. An earlier study has shown that a Polycomb group protein, Exh2, could assemble a methyltransferase complex in the cytoplasm of T cells (12) but Ezh2 was not characterized as a cytoplasm-specific isoform and its substrate in the cytoplasm is unknown. Here, we describe a cytoplasmic isoform of ATX1 containing only the SET domain (soloSET). We identified the elongation factor 1A (EF1A), its Lys396 (K396) in particular, as the cytoplasmic substrate for soloSET. Methylated lysines at this position are also found in maize and yeast (13,14) suggesting an evolutionary conservation of this modification in eukaryotic EF1A. However, whether/which lysines of the *Arabidopsis* EF1A protein are methylated has not been reported.

In addition to its roles in polypeptide chain elongation, eEF1A appears to be unique among all the translation factors by the diverse functions it has been ascribed outside of protein synthesis [reviewed in ref. (15)]. Due to its ability to bind and bundle actin, EF1A is considered a key factor in cytoskeleton organization (16–18). In plant cells actin bundling is used to build, position, and stabilize the main routes for organelle transport over long distances (19). Although methylated EF1A lysines have been connected to actin organization and bundling (13,14), the methyltransferases involved and the contribution of any particular methylated lysine are still unknown. Here, we show that methylation of the EF1A K396, located in the structural domain involved in actin bundling, is dependent on the activity of the SET domain encoded by the chromatin-modifying gene *ATX1*. This finding reveals an unsuspected role for a gene known so far to encode only an epigenetic factor.

MATERIALS AND METHODS

Arabidopsis thaliana ecotype Ws-2 and the earlier described *atx1* mutant line (5) were used. All primers

*To whom correspondence should be addressed. Tel: +1 402 472 3993; Fax: +1 402 472 2083; Email: zavramova2@unl.edu

The authors wish it to be known that, in their opinion, the first two authors should be regarded as joint First Authors.

used in this study are summarized in Supplementary Table S1.

Construction of GUS—expressing vectors and transgenic *Arabidopsis* lines

The Promoter-SET/*GUS (uidA)* (P_{SET}::GUS) reporter was constructed by cloning 476bp fragment upstream of the SET domain sequence using the *Pst*I containing forward and the *Nco*I containing reverse primers, respectively (Supplementary Table S1 and Figure S1). The product of the Taq polymerase PCR reaction (Invitrogen, http://www.invitrogen.com) was ligated into the pGEM-T vector system (PROMEGA, http://www.promega.com) and after sequence verification was sub-cloned into the pCambia1303 vector within the *Pst*I and *Nco*I sites, upstream of the β-Glucuronidase (Gus) gene. The P_{DIST}::GUS construct was cloned as above, except that the forward and reverse primers (Supplementary Table S1) amplified a 1026bp fragment further upstream (Supplementary Figure S1) to be tested as a promoter. The P_{ATX1}::GUS construct is described in ref. (20). Transgenic *Arabidopsis* lines expressing each of the constructs were generated by *Agrobacteria* mediated transformation (21) and transformed lines were selected for hygromycin resistance.

Construction of GFP-soloSET, GFP-EF1A, RFP-soloSET expression vectors and tobacco transient expression assays

GFP-soloSET and *RFP-soloSET* used in the transient expression assays were generated by recombining the pDONRT-SET vector with pB7FWG2.0 and pB7WGR2.0 expression vectors, respectively (22). *Agrobacteria* colonies containing binary plasmids for plant transformation were grown overnight in 10 ml of media with antibiotics. The cells were collected and re-suspended in an equal volume of induction medium (60 mM K_2HPO_4, 33 mM KH_2PO_4, $(NH_4)SO_4$, 1.7 mMNa Citrate•$2H_2O$, 10 mM MES, 1 mM $MgSO_4$, 0.2% glucose, 0.5% glycerol, antibiotics and 50 μg/ml of acetosyringone), and incubated with shaking for 6 h at 30°C. The cells were re-suspended to an OD_{600} of 0.8 in infiltration medium [0.5× MS, 10 mM *N*-moropholino-ethanesulfonic acid (MES), 150 μM Acetosyringone] and used for infiltrating the abaxial surface of *Nicotiana benthamiana* leaves. After 40 h, detection of expression was conducted by laser scanning confocal microscopy using 488- and 633-nm excitation and two-channel measurement of emission, 522 nm (green/GFP) and 680 nm (red/chlorophyll). RFP was detected by excitation at 540 nm and emission at 590 nm. Protein expression was confirmed by western blotting where necessary. In co-transformation experiments for GFP-soloSET with RNAi-SET or of GFP-EF1A with RFP-soloSET, equal volumes of *Agrobacteria* in infiltration medium, at OD_{600} of 0.8 were mixed and used for infiltration. Separate plants were used for control infiltrations.

Generation of transgenic plants expressing *RNAi-SET*

The SET domain of ATX1 was amplified using the gateway primers attB1SETFWD and attB2-ATX1. The PCR product was cloned by using the BP recombination reaction (Invitrogen) into the entry vector pDONRT207. After verifying the sequence integrity, the pDONRT-SET vector was recombined with the destination vector pFGC5941 (GenBank accession AY310901) by the LR reaction (Invitrogen) to generate the *RNAi* binary vector. The vector structure is illustrated in Supplementary Figure S2a. *RNAi-SET* transgenic *A. thaliana WS-2* lines were produced by *Agrobacteria tumefaciens* C58C1 mediated transformation (21). Transgenic lines were selected for basta resistance. The *RNAi-SET* effects were *ATX1* specific as mRNAs from two other SET domain genes, *ATX2* and *CLF*, were present in cells where *ATX1* transcripts were not detected (Supplementary Figure S2b).

Total RNA was extracted from the examined *Arabidopsis* plants using the TRIzol method (23). First-strand cDNA synthesis was preformed on 500 ng of RNA using the M-MLV System for RT–PCR (Invitrogen).

Two-dimensional gel electrophoresis and isoelectric focusing

Arabidopsis rosette leaves (0.3 g) were pulverized to a fine powder with liquid nitrogen with a mortar and pestle. Total protein extracts were prepared from the same samples that were used for mRNA purification by the TRIzol reagent (23). The proteins were re-suspended in 0.3 ml of isoelectric focusing (IEF) sample extraction media (8 M urea, 2 M thiourea, 2% [w/v] CHAPS, 2% [v/v] Triton X-100, 50 mM dithiothreitol) and were resolved in IEF and SDS-PAGE according to an established protocol (24) using the Bio-Rad system. Following SDS–PAGE, gels were washed in deionized water and stained with Coomassie or reacted with specific antibodies. Protein concentrations were determined using a protein assay Bio-Rad kit. Antibodies against ATX1 (raised in rabbit sera, GenScript, SC1031) and anti-trimethyl-H3K4 (Abcam, ab8580-100) were used. A Q-TOF Ultima tandem mass spectrometer (Waters) with electrospray ionization was used to analyze the eluting peptides.

Visualization of filamentous actin

Actin was labeled with rhodamine phalloidin following a recent protocol (25) with modifications. Leaves collected from 3-week-old *A. thaliana* plants were fixed with 4% paraformaldehyde freshly prepared in PEM buffer (100 mM PIPES, 10 mM EGTA, 5 mM $MgSO_4$, pH 6.9) for 1 h at room temperature, rinsed with wash buffer (0.1% Triton X-100 in PEM) and three times with PEM. The samples were treated with 1% cellulase (Sigma) and 1% driserase (Sigma) in PEM for 20 min at room temperature, rinsed with wash buffer and treated with 1% glycerol in wash buffer for 2 h. After rinsing with PEM, samples were stained with 100 nM rhodamine-phalloidin (Invitrogen, Molecular Probes, USA) in PEM for 30 min. After rinsing with wash buffer, samples were mounted on a glass slide in PEM and observed under a confocal microscope (model LSM510; Carl Zeiss).

For analyses of transcription factor binding motifs, information available in the database PLACE was used: http://www.dna.affrc.go.jp/PLACE/signalscan.html.

Mass spectrometry and data analysis

The stained bands were excised and subjected to LC/MS as described (26). Briefly, gel pieces were digested by trypsin (no.V5111, Promega, Madison, WI, USA) and digested peptides were extracted in 5% formic acid/50% acetonitrile and separated using C18 reversed phase LC column (75 micron × 15cm, Pepmap 300, 5 micron particle size) (Dionex, Sunnyvale, CA, USA). A Q-TOF Ultima tandem mass spectrometer (Waters) with electrospray ionization was used to analyze the eluting peptides. The system was user-controlled employing MassLynx software (v 4.1, Waters) in data-dependant acquisition mode with the following parameters: 0.9-sec survey scan (380–1900 Da) followed by up to three 1.4-s MS/MS acquisitions (60–1900 Da). The instrument was operated at a mass resolution of 8000. The instrument was calibrated using the fragment ion masses of doubly protonated Glu-fibrinopeptide. The peak lists of MS/MS data were generated using Distiller (Matrix Science, London, UK) using charge state recognition and de-isotoping with the other default parameters for Q-TOF data. Data base searches of the acquired MS/MS spectra were performed using Mascot (Matrix Science, v1.9.0, London, UK). The NCBI non-redundant database (2 010 130–10 386 837 sequences 3 543 419 944 residues) was used restricted to *A. thaliana*. Search parameters used were: no restrictions on protein molecular weight or pI, enzymatic specificity was set to trypsin with up to three missed cleavage sites, carbamidomethylation of C was selected as a fixed modification, and methionine oxidation along with mono-, di- and trimethylation of lysine were allowed as variable peptide modifications. Mass accuracy settings were 0.15 Da for peptide mass and 0.12 Da for fragment ion masses.

RESULTS

A soloSET domain isoform is generated from an internal promoter in the *ATX1* locus

In addition to the full-size ATX1 protein, immunoblot assays of total protein extracts from wild-type *Arabidopsis* leaf cells with anti ATX1-antibodies consistently revealed presence of a lower-size ~22 kDa protein band (Figure 1a). N-terminal Edman sequencing identified the sequence MNTPSNIL, which matches the 5′-end of the SET domain, indicating that the 22 kDa protein band represents the SET domain of ATX1. Unexpectedly, this band was present also in blots from the *atx1* mutant cells (Figure 1b). As the T-DNA insertion in the *atx1* mutant line disrupts the *ATX1* mRNA (Figure 1c), the 22 kDa protein from the C-terminal gene region in *atx1* cells apparently originated from a message generated downstream of the insertion (Figure 1b–d). To test for the existence of a promoter that could account for such a message, we mapped various transcripts from the *ATX1* region.

Primers overlapping regions upstream of the *T*-DNA insertion amplified the expected bands from both wild-type and *atx1* mutant cells illustrating presence of messages from the sequences in the N-terminal half of the gene (Figure 1c and d panels Tu-DAST, Tu-PWWP and DAST). However, sequences flanking the *T*-DNA insertion site were amplified only from WT mRNA but not from the *atx1* template (panel DAST-PHD). Similarly, specific primers overlapping sequences downstream of the insertion site amplified a band only from the wild type (panel PHD-SET). However, primers specific for the SET domain revealed presence of transcripts from both the WT and the *atx1* samples (panel SET) supporting

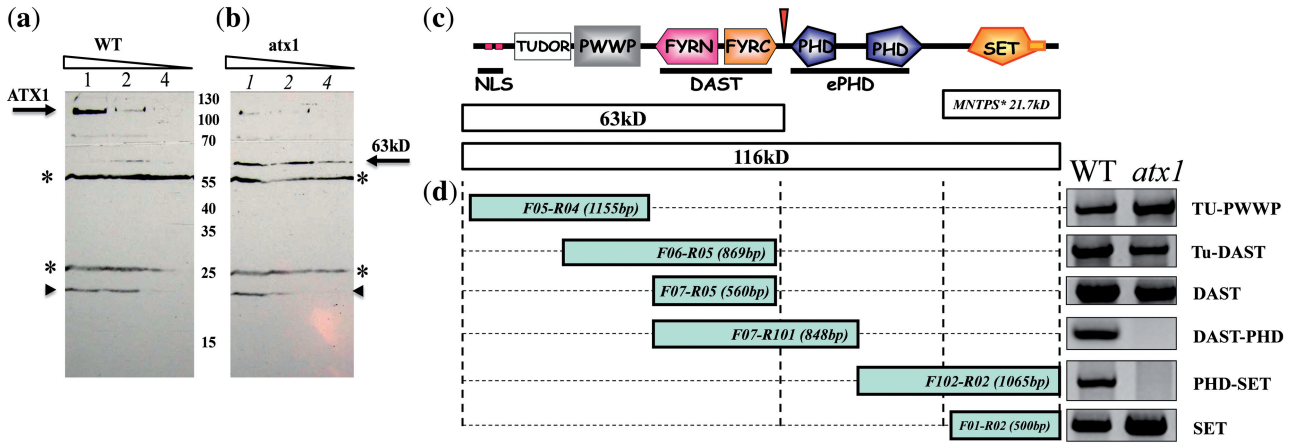

Figure 1. SoloSET isoform produced from an internal *ATX1* promoter. (**a**) Western blots of total cellular extracts from WT cells with the antiATX1 antibody. The 116 kDa corresponding to full-size ATX1 is indicated by an arrow. The 22 kDa (soloSET) protein band is indicated by the arrowhead. Sample dilutions (0-, 2-, 4-fold) are indicated on top of lanes. Two nonspecific signals are marked with asterisks. (**b**) Western blot analysis of total cellular extracts from *atx1* leaf cells with antiATX1 antibody. The ~63 kDa protein band (indicated by arrow) apparently represents a truncated protein. The 22 kDa soloSET protein is indicated by the arrowhead. Other annotations are as in (a). (**c**) Schematic representation of the *ATX1* locus. The site of *Ti*-DNA insertion on *atx1* mutants is shown by the black triangle. The empty boxes under the gene indicate the size of protein products generated from the gene. (**d**) Tested regions amplified with specific primers. The boxes represent the size of the expected bands amplified with the primers indicated in the boxes (Supplementary Table S1).

the existence of a promoter that drives transcription from SET sequences separately from their transcription in the context of the full *ATX1* mRNA.

To validate the existence of such a promoter by another approach, a DNA region upstream of the MNTPSNILS sequence was tested as a promoter for the *GUS* gene (P_{SET}::GUS in Supplementary Figure S1a and b). A 1024 bp DNA sequence from a region further upstream, carrying a putative TATA-box (the distal promoter) was also tested for promoter activity (P_{DIST}::GUS). Transgenic lines stably expressing each of these constructs revealed that P_{SET} drove *GUS* expression in all twelve independently transformed lines indicating that the 0.5 kb DNA upstream of SET does function as a promoter (Supplementary Figure S3a and b). In contrast, the distal ~1 kb sequence did not activate *GUS* expression (11 P_{DIST}::GUS lines were analyzed) despite the presence of a TATA-box like sequence. Comparing lines expressing *GUS* under the native promoter for the full-size *ATX1* gene (P_{ATX1}::GUS) revealed partially overlapping expression domains and some differences as well (Supplementary Figure S3a and c; 15). P_{SET}::GUS was strongly expressed in young seedlings, while P_{ATX1}::GUS staining was strong in cotyledons, but weak in the first true leaves, except at the hydothodes. Later in development, P_{SET}::GUS narrowed its expression domains but remained prominent in cells at attachment sites of organ to stems; *ATX1* is ubiquitously expressed, particularly strong in the vasculature of leaves and stems (Supplementary Figure S3b and c; 15). Collectively, our results indicate that a *bona fide* promotor exists upstream of the SET-ATG codon driving strong *SET* mRNA expression in cells, particularly at the sites of organ attachment.

Comparative analysis of the putative transcription factor-binding sites at the *ATX1* and soloSET promoters using the PLACE database ('Materials and Methods' section) revealed a larger number of putative TF-binding sites upstream of *ATX1* suggesting that *ATX1* could be subjected to a broader array of regulatory signals than soloSET. However, shared putative binding sites for factors regulated by abiotic stress and hormonal signals were also recognized.

Subcellular localization of soloSET and effects of *RNAi-SET* expression

Transient expression of a soloSET-GFP fusion protein in tobacco leaf cells revealed that it was present only in the cytoplasm (Figure 2a). This is in contrast to ATX1-GFP, which localizes in the nucleus (Figure 2b) but dynamically shifts between the nucleus and the cytoplasm in response to signals (27). To asses a possible role of soloSET, we constructed transgenic lines expressing *RNAi-SET*. Transgenic plants displayed strong phenotypes: precocious flowering (occurring at a stage with only four true leaves), asymmetric rosettes (note different sizes of leaves 3 and 4), aberrant flowers and chlorosis (Figure 2c). Aberrant flowers and precocious flowering were displayed also by *atx1* mutants (5), although never as early as at a four-leaf stage. Also, we have not observed chlorosis under normal watering and long day conditions in *atx1* mutants. Despite these perceived differences, however, we concluded that the visible phenotypes, alone, could not be reliable indicates of soloSET function. Consequently, we focused on determining its role at the cellular and molecular levels.

First, we asked whether *RNAi-SET* affected the levels of *ATX1* and/or *soloSET* transcripts. Using primers overlapping various regions of the *ATX1* gene, we show the results from six independently transformed lines analyzed by RT–PCR (Figure 3a and b). As expected, the primers failed to amplify all regions in the *ATX1* mRNA, except at the 3′-end. An exception was line 4 where weak bands were detected from amplification of regions upstream of the *Ti*-insertion. Most unexpected, however, was the recovery of the SET-domain sequences from all transgenic samples indicating that SET domain transcripts were produced in all *RNAi-SET* lines (Figure 3a). These results indicated that production of *ATX1* transcripts was knocked down in the presence of *RNAi-SET*, while transcripts from its SET-domain region (*soloSET*) were not substantially decreased.

To pursue further the fate of the *soloSET* messages we examined the *RNAi-SET* effects on the production of soloSET protein. To this end, total protein extracts from WT cells were resolved by two-dimensional (2D) gel electrophoresis and reacted with antiATX1 antibodies. The full-size ATX1 and the soloSET proteins produced in wild-type cells are shown (Figure 4a). The nature of the spots indicated by the arrowhead and the arrow was confirmed by mass spectroscopy (MS) (Supplementary Figure S4a and b). In western blots of extracts from *RNAi-SET* expressing cells both spots were missing indicating that neither ATX1 nor soloSET were produced (Figure 4a). A few other proteins reacting non-specifically with the ATX1 antibody retained their signals in the *SET-RNAi* sample illustrating that the *RNAi-SET* effects upon ATX1 and soloSET were specific. The results indicate

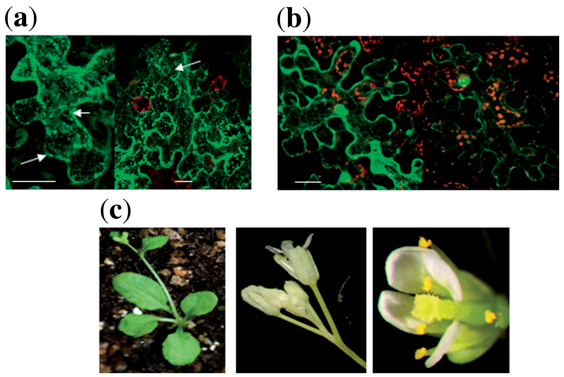

Figure 2. Cytoplasmic localization of soloSET and transgenic plants expressing *RNAi-SET*. (**a**) Transiently expressed GFP-soloSET fusion protein in tobacco leaf cells is detected only in cytoplasm. Arrows point to perinuclearly localized green signal. (**b**) Nuclearly localized full-size ATX1-GFP fusion protein is shown for comparison. Chloroplasts are shown in red (chlorophyll autoflorescence). Bars are 20 μm. (**c**) transgenic *Arabidopsis* plants expressing *RNAi-SET* showing precocious flowering (at the stage of only four true leaves), chlorosis in sepals and inflorescences, and a flower with abnormal short stamen (arrowhead) and asymmetric petals (arrows).

that, ultimately, in the presence of *RNAi-SET*, production of both ATX1 and soloSET is suppressed but suppression is achieved by different mechanisms: by knocking down *ATX1* transcripts but by disrupting the production of the soloSET protein from its transcripts. What determines the different modes of ATX1 and soloSET suppression by *SET-RNAi* remains to be elucidated but it is tempting to speculate that they reflect different mechanisms regulating the production of the full-size ATX1 and of its shorter soloSET version.

The ability of *RNAi-SET* to suppress soloSET was confirmed also by an independent approach. A *soloSET-GFP* fusion construct produced a strong fluorescent signal when expressed alone in tobacco cells (Figure 4b). However, the signal was completely eliminated when *soloSET-GFP* and *RNAi-SET* were co-transformed (Figure 4c). We conclude that soloSET-GFP production was effectively suppressed by *RNAi-SET*.

SoloSET interacts with EF1A

In an earlier screening of a yeast-two-hybrid expression library with the SET-domain sequence as bait, we have identified the cDNA from the *At5g60390* gene as a SET-domain binding candidate. *At5g60390* encodes the elongation factor 1A (EF1A) and, here, we tested the interaction of the two proteins by the pull-down assay. A GST-SET fusion protein was produced, immobilized on a column and reacted with protein extracts from wild-type leaf cells. A band of ~50 kDa, corresponding to the molecular size of the *Arabidopsis* EF1A protein (Figure 5a), was detected by immunoblotting with antibodies against the maize protein. The band was positively identified as EF1A by MS (Supplementary Figure S5). We note that the SET-peptide selectively picked EF1A amongst the proteins present in whole cellular extracts confirming, thus, the interaction of EF1A and SET-ATX1 and their strong preference for each other as binding partners.

Next, we asked whether the two proteins interact in plant cells. We co-expressed RFP-tagged soloSET and GFP-tagged EF1A in tobacco cells and detected that they co-localize in the cytoplasm (Figure 5b). As also shown in earlier reports (28,29), the *Arabidopsis* EF1A localized in the nuclei as well. However, the soloSET co-localized with EF1A only on the nuclear periphery but not in the nuclei (Figure 5b, inset) supporting the conclusion that that the two proteins interact only in the cytoplasm.

SoloSET is required and sufficient for methylation of EF1A

Known bacterial EF-Tu (30) and eukaryotic eEF1A (yeast, fungi, animals and plants) are posttranslationally methylated (13,31–33). However, the methyltransferases

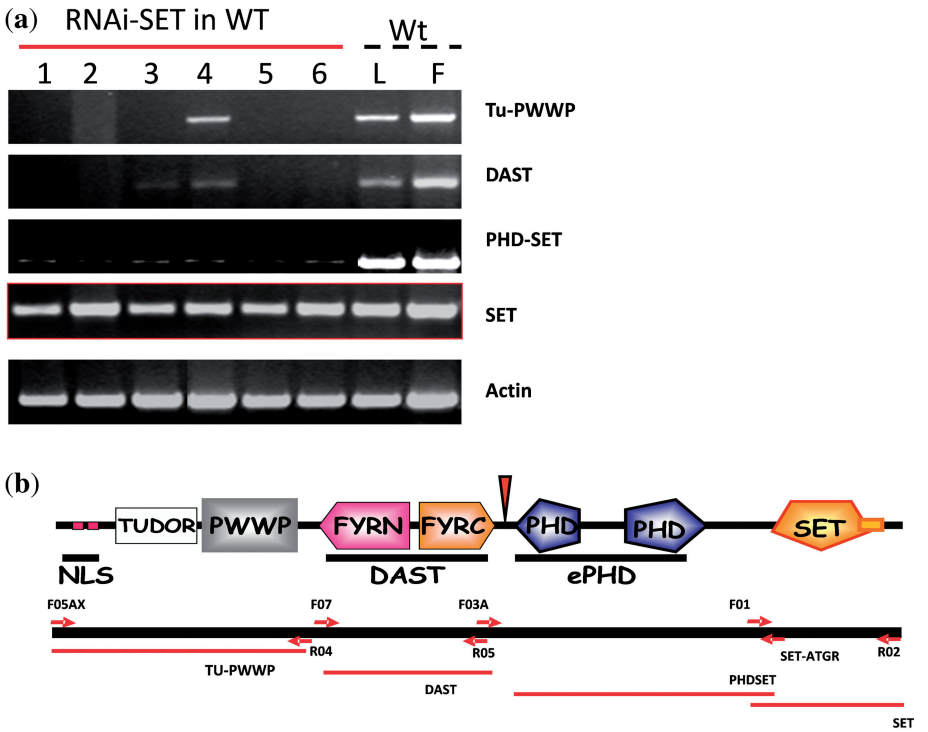

Figure 3. Transcripts produced from the *ATX1* locus in *RNAi- SET* transformed plants. (**a**) RT–PCR analysis of *ATX1* specific transcripts. The peptide domains encoded by the tested regions are shown to the right of the panels. Numbers of top of lanes indicate independently transformed lines tested for expression of ATX1 and its derivatives. As controls, all primers were tested for the specific fragment amplification in wild-type leaf (L) and flower (F) tissues. SET domain transcripts detected in all transgenic lines are shown in the panel indicated as SET. Transcripts from upstream ATX1 regions were not detected, except for weak bands corresponding to the Tu-PWWP and DAST regions in line 4. (**b**) Positioning of the primers used to amplify specific regions and of the produced transcripts are illustrated.

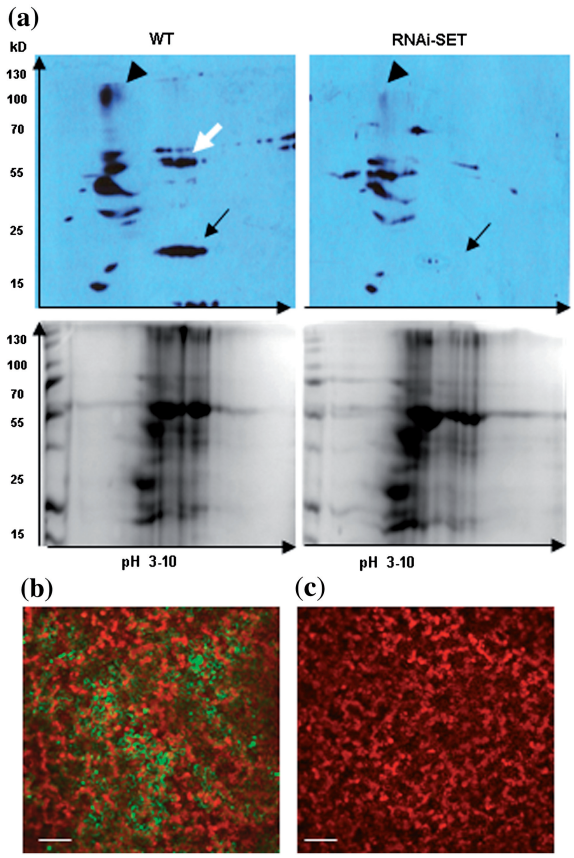

Figure 4. *RNAi- SET* expressing cells inhibit synthesis of ATX1 and soloSET proteins. (**a**) Two-dimensional-electrophoretically resolved proteins from WT and *RNAi-SET* expressing cells followed by immunostaining with the antiATX1 antibody. Full-size ATX1 (arrowhead), soloSET (arrow) and an apparently degradation product (white arrow) are present only in the WT. Proteins non-specifically binding the antiATX1 antibody were not detectably affected. The two bottom panels are Coomassie stained gels run in parallel with the top pair. MW scale is shown on the vertical coordinate. Horizontal arrows show the pH gradient. (**b**) GFP-soloSET fusion protein transiently expressed in tobacco leaf cells. Chloroplasts are shown in red as a background for transformed cells (green). (**c**) *RNAi-SET* co-transformed with GFP-soloSET eliminated the GFP-signal consistent with a suppressed production of soloSET. Bars are 50 μM.

involved have not been identified. It is also unknown which, if any, of the *Arabidopsis* EF1A lysine residues are methylated. The binding of soloSET to EF1A hinted at the intriguing possibility that soloSET might play a role in methylating EF1A.

Using C^{14}-labeled SAM as donor and recombinantly produced soloSET and EF1A proteins, we were unable to detect a methylated EF1A product. Likewise, recombinantly expressed ATX1 is unable to effectively methylate its histone target *in vitro* (5). Consequently, we examined whether soloSET was involved in EF1A methylation *in vivo*. Our approach was based on the serendipitous finding that antibodies against trimethylated lysine 4 of histone H3 (H3K4me3), but not against H3K4me2 or H3K9me2, detected methylated EF1A. We note that the H3K4me3 antibodies are used here only as a tool to detect EF1A methylation and not to imply specificity for any methylated lysine; it is noted also, that the H3K4me3 antibodies reacted with a few other unidentified proteins.

Cellular extracts from WT and from *RNAi-SET* transgenic plants were resolved by 2D gel electrophoresis and the spot corresponding to EF1A (Figure 5c, arrow in left-hand panel) was excised and positively identified as EF1A by MS. Importantly, EF1A was produced in *RNAi-SET* cells (Figure 5c, arrow in right-hand panel). However, there was a notable difference in the EF1A methylation states in *RNAi*-SET versus wild-type cells. The signal from EF1A in transgenic cells was absent (Figure 5d, arrow) indicating loss of EF1A methylation. The signals from the other non-specific proteins remained largely unchanged providing evidence that depletion of SET domain activity affected specifically the methylation of EF1A. We note also that ATX1 disruption in *atx1* cells did not eliminate methylation of EF1A (Figure 5e) although it abolished ATX1 function at chromatin (8,20). As soloSET is produced in the *atx1* background, the result indicates that the SET domain, alone, is necessary and sufficient for EF1A methylation.

Mass spectroscopy was used to identify the methylated residues. Analyses of the spots corresponding to EF1A from WT cells detected mono-methylated K261, dimethylated K55 and tri-methylated K79, K187 K306, and K396 (Supplementary Figure S6a). The same modified lysines were identified again in the *RNAi-SET* expressing sample, with the notable exception of K396 (Supplementary Figure S6b). This result defines Lys396 as the specific target. The loss of the three-methyl groups suggested that the ATX1-derived SET was involved in modifying K396 at all three positions of the amino group, unlike ATX1, which mainly affects tri-methylation of H3K4 in chromatin (8). These results, reproduced in three independent experiments, confirm that EF1A–K396 is specifically modified by the SET domain.

The validity of our MS results for the *Arabidopsis* EF1A is further supported by the pattern of lysine methylations reported for the maize EF1A: tri-methylated K79, K187, K306 and monomethylated K396 (13). The results indicate that lysine methylations at these positions are conserved in the monocot and dicot lineages. Even more significant is the finding of a tri-methylated K390 in the yeast EF1A, corresponding to the K396 of plants' EF1A (14), as it suggested an evolutionarily conserved role for the methylation of this residue in EF1A. K396 is located in the domain involved in the EF1A actin bundling, the best studied non-canonical function of elongation factors (14–18). In yeast, substitution of the post-translationally modified lysines with arginines did not affect translation but altered actin cytoskeleton organization (14). Next, we examined whether loss of K396 methylation resulting from soloSET suppression had any effect on actin filament patterns in *Arabidopsis* cells.

Actin cytoskeleton in *RNAi-SET* and in *atx1* mutant cells

Consistent with available data, actin in wild-type leaf cells was observed at the plasma membrane (cortical actin) and

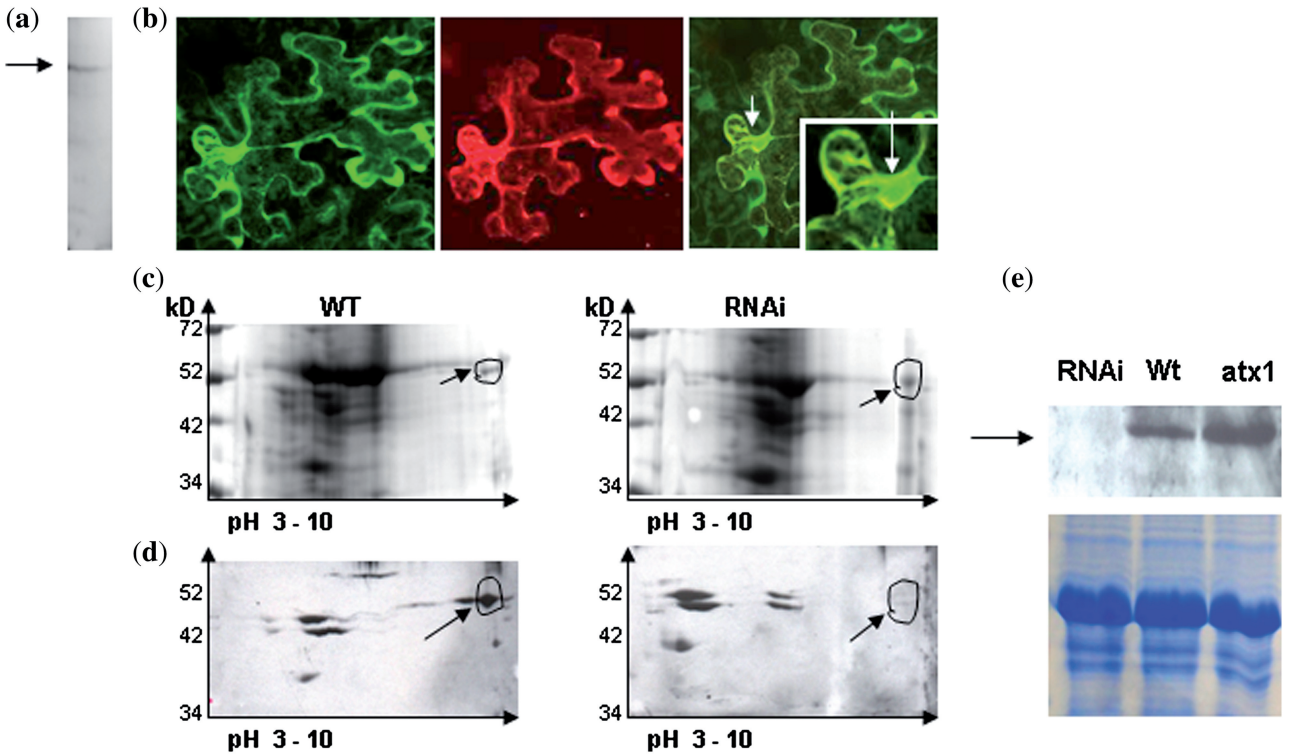

Figure 5. Interaction of the SET domain with eEF1A. (**a**) GST-SET pull-down of total protein extract from WT *Arabidopsis* leaves followed by immunoreaction with the maize antiEF1A antibody. The 50 kDa protein corresponds to the *Arabidopsis* EF1A (arrow). (**b**) Transiently co-expressed GFP-EF1A (green) and RFP-soloSET (red) fusion proteins in tobacco leaf cells. Overlapping signals appear in yellow. Arrows point to nuclei. (**c**) Two-dimensonal-distribution of proteins from WT and from *RNAi-SET* (RNAi) expressing cellular extracts (Coomassie blue staining). Arrows point to the EF1A spot, isoelectric point 9.20. (**d**) Immunostaining of the 2D-gel blots with the antibody against H3K4me3. (**e**) Western blots of protein extracts from *SET-RNAi*, WT and *atx1* cells with the antiH3K4me3 antibody. Arrow indicates position of the 50 kDa protein band. Coomassie-stained proteins are shown as loading controls in the lower panel.

as fine and thick bundled actin networks (Figure 6a–c). Longitudinal, transverse, and randomly oriented actin bundles, considered general features of interphase plant cells (19), are clearly displayed. The transvacuolar cytoplasmic strands (TVSs) providing direct connections between different regions in the cytoplasm are also prominent in wild-type cells. In contrast, *RNAi-SET* expressing cells displayed a dramatically different pattern of reduced actin bundles and absent TVSs (Figure 6e–j). The fluorescent signal is associated mostly with particulate structures at the vacuolar periphery suggesting a collapse of the bundled structures. These changes were displayed by all *RNAi-SET* expressing cells implicating SET-domain activity in the actin bundling in *Arabidopsis* cells. In sharp contrast, actin bundles and TVSs similar to the wild type were prominently displayed in *atx1* mutant cells (Figure 6k–m).

These results are important because they indicate that loss of ATX1 function does not alter the actin cytoskeleton. Thereby, the cytoskeletal phenotype is dependent on presence of functional SET, but not ATX1, illustrating a critical distinction of the roles played by the two isoforms. As soloSET is produced in the *atx1* background (Figure 1b), it is logical to conclude that actin bundling is dependent on the activity carried by soloSET, most likely, through its role in methylating EF1A K396. This residue is located in the actin-binding domain (III) of EF1A and its methylation state might be critical for the interaction. Observations that amino acid mutations in the yeast EF1A domain III resulted in disappearance of actin cables and appearance of granular actin patches (17), while substitution of the methylated lysines with arginines altered actin cytoskeleton organization in yeast (14) support this possibility.

DISCUSSION

Collectively, our results provide answers to two currently open and, apparently, unrelated questions: whether chromatin modifying (epigenetic) genes encode factors that modify proteins other than the histones and what methyltransferases are involved in modifying the EF1A lysines.

We provide an example of an isoform of an epigenetic factor with a role unrelated to chromatin. It is also the first example of a Trithorax family member produced from an internal gene promoter.

Three independent types of evidence distinguish SET function as part of ATX1 and as a solo domain: first, the two products of the *ATX1* gene are localized in different cellular compartments; second, a disrupted ATX1 (in *atx1* cells, where soloSET is produced) did not eliminate methylation of EF1A (Figure 5e) but H3K4 methylation

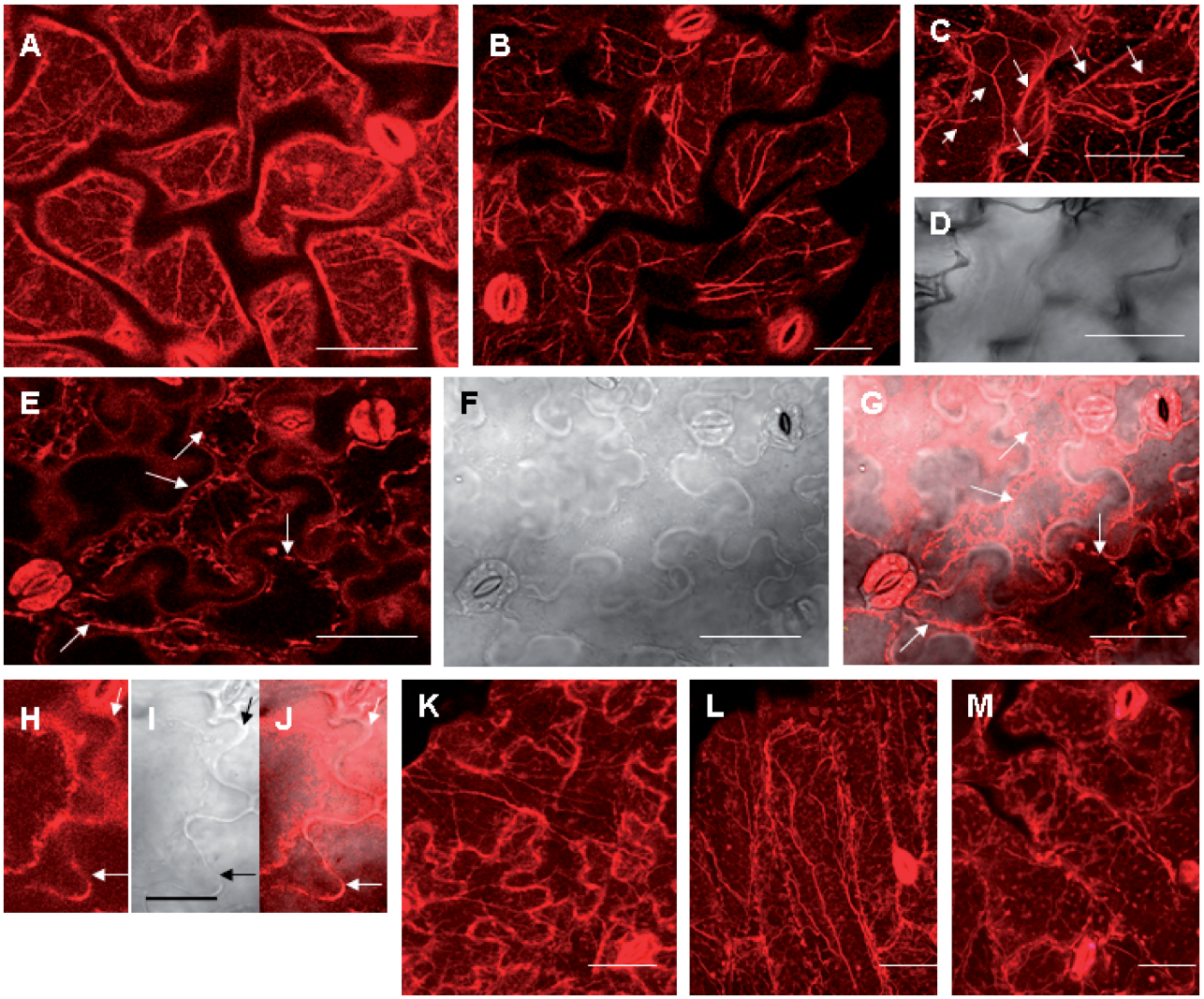

Figure 6. The actin cytoskeleton and *RNAi-SET*. Actin filaments stained with phalloidin in wild-type leaf cells exhibiting actin bundles of various thicknesses (**a–c**). A contrast image (**d**) of the cells shown in (**c**) illustrating the TVS (arrows). Bars are 20 μM. Actin filaments in *RNAi-SET* expressing cells in (**e–j**). Granular particles on the vacuolar periphery are indicated by arrows in e. (g) Bars are 20 μM. Closer look at vacuolar-associated actin (h–j). Arrows indicate the cell wall. Bar is 10 μM. Actin bundles in *atx1* mutant cells (**k–m**). Bars are 20 μM.

at ATX1 chromatin targets was erased (3,8,20). As presence of SET domain alone it is not sufficient for the methylation of H3K4 but is sufficient for the methylation of EF1A, it indicates that the SET domain peptide plays different roles when alone and as part of the ATX1 protein; third, loss of SET, but not of the histone modifying ATX1-SET activity (in the *atx1* background) affects cytoskeletal actin bundling and the cytoplasm-specific phenotype. Our results do not exclude the possibility that SET within ATX1 could also modify K396, a function that would be redundant with soloSET. However, given that deletion of SET from ATX1 (in *atx1* mutants) does not affect the EF1A associated functions, indicates that the role of ATX1 is not essential for these cytoplasmic functions. We consider these results among the most significant findings of this study as it has been known for a number of years that some EF1A lysines are methylated, that methylation of specific lysines is evolutionarily conserved, and that these modifications are involved in cytoskeletal functions (actin bundling) rather than in protein synthesis. However, the methyltransferases modifying the EF1A lysines and whether distinct enzymes modify specific lysines have been hitherto unknown. Here, we have identified the first methyltransferases involved in the methylation of EF1A and have shown that it modifies specifically one, among several, methylated lysines. Thereby, it is logical to expect that different methyltransferases modify specific lysines, which regulate (or reflect) the broad spectrum of roles of the multitasking EF1A. It is tempting to speculate that lysine-specific methylation in EF1A play roles similar to the roles played by the specific histone marks on chromatin. Furthermore, the methylated lysines of the *Arabidopsis* EF1A identified in our study and, particularly, the conserved K396 methylation, were also found in a monocot and in yeast providing a strong argument for

an evolutionarily conserved importance for this modification.

Lastly, we note that soloSET provides an example of a eukaryotic SET domain protein structurally similar to the SET domain proteins found in bacteria. Despite a belief that *SET* domain genes have occurred with eukaryotes (34,35), phylogenetic analysis has suggested that the genes are ancient and do not result from a lateral gene transfer (36). Protein methylating activity was reported for a *M. mazei* SET domain protein (37) but the role of the bacterial SET domain proteins remains unknown. Demonstrating that SET domain proteins have roles outside the nucleus might trigger exploration of their function in prokaryotes and stimulate discovery of novel cytoplasmic functions produced by genes known currently to encode only chromatin modifiers.

SUPPLEMENTARY DATA

Supplementary Data are available at NAR Online.

ACKNOWLEDGEMENTS

The authors gratefully acknowledge R. Alvarez-Venegas (CINVESTAV-IPN Irapuato, Mexico) the yeast-two-hybrid screening contribution and to B. Larkins (U. Arizona) for the gift of the antibody against the maize EF1A. The authors are grateful to C. Elowski and J. Zou (UNL) and to H. Gabrys (Silesian University). As experts in actin cytoskeleton in animal, as well as plant cells, they provided valuable comments, insights and helpful suggestions. Edman degradation was done at UNOMC Protein Structure Core Facility.

FUNDING

National Institutes of Health award P20 RR15635 (to MS facility), National Institutes of Health award RR015468-01; NSF-EPS0701892, partial (to Z.A.); NSF-MCB0749504, partial (to Z.A.). Funding for open access charge: NSF-MCB0749504.

Conflict of interest statement. None declared.

REFERENCES

1. Qian,C. and Zhou,M.M. (2006) SET domain protein lysine methyltransferases: Structure, specificity and catalysis. *Cell Mol. Life Sci.*, **63**, 2755–2763.
2. Kouzarides,T. (2007) Chromatin modifications and their function. *Cell*, **128**, 693–705.
3. Avramova,Z. (2009) Evolution and pleiotropy of TRITHORAX function in Arabidopsis. *Int. J. Dev. Biol.*, **53**, 371–381.
4. Eissenberg,J.C. and Shilatifard,A. (2010) Histone H3 lysine 4 (H3K4) methylation in development and differentiation. *Dev. Biol.*, **339**, 240–249.
5. Alvarez-Venegas,R., Pien,S., Sadder,M., Witmer,X., Grossniklaus,U. and Avramova,Z. (2003) An *Arabidopsis* homolog of Trithorax has histone methylase activity and activates flower homeotic genes. *Curr. Biol.*, **13**, 627–637.
6. Alvarez-Venegas,R., Al-Abdallat,A., Guo,M., Alfano,J. and Avramova,Z. (2007) Epigenetic Control of a Transcription Factor at the Node of Convergence of Two Signaling Pathways. *Epigenetics*, **2**, 106–113.
7. Ding,Y., Lapko,H., Ndamukong,I., Xia,Y., Al-Abdallat,A., Lalithambika,S., Sadder,M., Saleh,A., Fromm,M., Riethoven,J.-J. *et al.* (2009) The Arabidopsis chromatin modifier ATX1, the myotubularin-like AtMTM and the response to drought. *Plant Signal. Behav.*, **4**, 1049–1058.
8. Alvarez-Venegas,R. and Avramova,Z. (2005) Methylation patterns of histone H3 Lys 4, Lys 9 and Lys 27 in transcriptionally active and inactive Arabidopsis genes and in *atx1* mutants. *Nucleic Acids Res.*, **33**, 5199–5207.
9. Alvarez-Venegas,R. and Avramova,Z. (2001) Two *Arabidopsis* homologs of the animal *trithorax* genes: a new structural domain is a signature feature of the trithorax gene family. *Gene*, **271**, 215–221.
10. Alvarez-Venegas,R. and Avramova,Z. (2002) SET-domain proteins of the Su(var), E(z) and T*rithorax* families. *Gene*, **285**, 25–37.
11. Veerappan,C.S., Avramova,Z. and Moriyama,E. (2008) Evolution of SET-domain protein families in the unicellular and multicellular Ascomycota fungi. *BMC Evol. Biol.*, **8**, 190.
12. Su,I.H., Dobenecker,M.W., Dickinson,E., Oser,M., Basavaraj,A., Marqueron,R., Viale,A., Reinberg,D., Wülfing,C. and Tarakhovsky,A. (2005) Polycomb group protein Ezh2 controls actin polymerization and cell signaling. *Cell*, **121**, 425–436.
13. Lopez-Valenzuela,J.A., Gibbon,B.C., Hughes,P.A., Dreher,T.W. and Larkins,B.A. (2003) eEF1A isoforms change in abundance and actin-binding activity during maize endosperm development. *Plant Physiol.*, **133**, 1285–1295.
14. Cavallius,J., Popkie,A.P. and Merrick,W.C. (1997) Site-directed mutants of post-translationally modified sites of yeast eEF1A using a shuttle vector containing a chromogenic switch. *Biochim. Biophys. Acta*, **1350**, 345–358.
15. Mateyak,M.K. and Kinzy,T.G. (2010) eEF1A: Thinking othe ribosome. *J. Biol. Chem.*, **285**, 21209–21213.
16. Condeelis,J. (1995) Elongation factor 1 alpha, translation and the cytoskeleton. *Trends Biochem. Sci.*, **20**, 169–170.
17. Gross,S.R. and Kinzy,T.G. (2005) Translation elongation factor 1A is essential for regulation of the actin cytoskeleton and cell morphology. *Nat. Struct. Mol. Biol.*, **12**, 772–778.
18. Owen,C.H., DeRosier,D.J. and Condeelis,J. (1992) Actin crosslinking protein EF-1a of *Dictyostelium discoideum* has a unique bonding rule that allows square-packed bundles. *J. Struct. Biol.*, **109**, 248–254.
19. Thomas,C., Tholl,S., Moes,D., Dieterle,M., Papuga,J., Moreau,F. and Steinmetz,A. (2009) Actin bundling in plants. *Cell Motil. Cytoskeleton*, **66**, 940–957.
20. Saleh,A., Alvarez-Venegas,R., Yilmaz,M., Le,O., Al-Abdallat,A. and Avramova,Z. (2008) The highly similar *ARABIDOPSIS HOMOLOGS OF TRITHORAX ATX1* and *ATX2* encode divergent biochemical functions. *Plant Cell*, **20**, 568–579.
21. Clough,S.J. and Bent,A.F. (1998) Floral dip: a simplified method for *Agrobacterium*-mediated transformation of *Arabidopsis thaliana*. *Plant J.*, **16**, 735–743.
22. Karimi,M., Inze,D. and Depicker,A. (2002) Gateway vectors for *Agrobacterium*-mediated plant transformation. *Trends Plant. Sci.*, **7**, 193–195.
23. Chomczynski,P. (1993) A reagent for the single-step simultaneous isolation of RNA, DNA and proteins from cell and tissue samples. *Biotechniques*, **15**, 532–534, 536–537.
24. Hajduch,M., Ganapathy,A., Stein,J. and Thelen,J.A. (2005) Systematic proteomic study of seed filling in soybean. Establishment of high-resolution two-dimensional reference maps, expression profiles, and an interactive proteome database. *Plant Physiol.*, **137**, 1397–1419.
25. Era,A., Tominaga,M., Ebine,K., Awai,C., Saito,C., Ishizaki,K., Yamato,K.T., Kohch,K., Nakano,A. and Ueda,T. (2009) Application of Lifeact Reveals F-Actin Dynamics in *Arabidopsis thaliana* and the Liverwort. *Marchantia polymorpha - Plant Cell Physiol.*, **50**, 1041–1048.

26. Kayser,J.P., Vallet,J.L. and Cerny,R.L. (2004) Defining parameters for homology tolerant database searching. *Biomol. Tech.*, **15**, 285–295.
27. Alvarez-Venegas,R., Sadder,M., Hlavacka,A., Baluška,F., Xia,Y., Firsov,A., Sarath,G., Moriyama,H., Dubrovsky,J. and Avramova,Z. (2006) The Arabidopsis Homolog of Trithorax, ATX1, binds phosphoinositide 5-phosphate and the two regulate a common set of target genes. *Proc. Natl Acad. Sci. USA*, **103**, 6049–6054.
28. Koroleva,O.A., Tomlinson,M.L., Leader,D., Shaw,P. and Doonan,J.H. (2005) High-throughput protein localization in Arabidopsis using Agrobacterium-mediated transient expression of GFP-ORF fusions. *Plant J.*, **41**, 162–74.
29. Ruepp,A., Zollner,A., Maier,D., Albermann,K., Hani,J., Mokrejs,M., Tetko,I., Güldener,U., Mannhaupt,G., Münsterkötter,M. *et al.* (2004) The FunCat, a functional annotation scheme for systematic classification of proteins from whole geneomes. *Nucleic Acid Res.*, **32**, 5539–5545.
30. Kraal,B., Lippmann,C. and Kleanthous,C. (1999) Translational regulation by modifications of the elongation factor Tu. *Folia Microbiol.*, **44**, 131–141.
31. Cavallius,J., Zoll,W., Chakraburtty,K. and Merrick,W.C. (1993) Characterization of yeast EF-1 alpha: non-conservation of post-translational modifications. *Biochim. Biophys. Acta*, **1163**, 75–80.
32. Fonzi,W.A., Katayama,C., Leathers,T. and Sypherd,P.S. (1985) Regulation of protein synthesis factor EF-1 alpha in *Mucor racemosus*. *Mol. Cell. Biol.*, **5**, 1100–1103.
33. Kristensen,P., Lund,A., Clark,B.F., Cavallius,J. and Merrick,W.C. (1998) Purification and characterization of a tissue specific elongation factor 1 alpha (EF-1 alpha 2) from rabbit muscle. *Biochem. Biophys. Res. Commun.*, **245**, 810–814.
34. Aravind,L. and Iyer,L.M. (2003) Provenance of SET-domain histone methyltransferases through duplication of a simple structural unit. *Cell Cycle*, **2**, 369–376.
35. Stephens,R.S., Kalman,S., Lammel,C., Fan,J., Marathe,R., Aravind,L., Mitchell,W., Olinger,L., Tatusov,R.L., Zhao,Q. *et al.* (1998) Genome sequence of an obligate intracellular pathogen of humans: Chlamydia trachomatis. *Science*, **282**, 754–759.
36. Alvarez-Venegas,R., Tikhonov,A., Sadder,M. and Avramova,Z. (2007) Origin of the bacterial SET domain genes: vertical or horizontal? *Mol. Biol. Evol.*, **24**, 482–497.
37. Manzur,K.L. and Zhu,M.M. (2005) An archaeal SET domain protein exhibits distinct methyltransferase activity towards DNA-associated protein MC1-a. *FEBS Lett.*, **579**, 3859–3865.

Supplemental Table 1 (SI Table 1) Primers used for the various cloning procedures

Primer	5'-Sequence-3'	Purpose
attB-1EF1a	GGGGACAAGTTTGTACAAAAAAGCAGGCTTAATGGG TAAAGAGAAGTTT	Forward primer for PCR amplification of EF1a gateway sequence
attB1-SETFWD	GGGGACAAGTTTGTACAAAAAAGCAGGCTTAATGAA TACTCCAAGCAACATTCTTT	Forward primer for PCR amplification of solo-SET gateway sequence
attB2-ATX1	GGGGACCACTTTGTACAAGAAAGCTGGGTCTTCTGCG GTCCAGTCTATTAG	Reverse primer for PCR amplification of solo-SET gateway sequence
attB2-EF1a	GGGGACCACTTTGTACAAGAAAGCTGGGTATCATGTC CCTAACAGCGAA	Reverse primer for PCR amplification of EF1a gateway sequence
ATX1-F01	GGAAGAGATTAGCATTTGGG	Forward primer from the beginning of the SET domain
ATX1-F03A	TGTCCGTGTTGACTGGAAAGATCTC	Forward PCR primer from the end of the DAST domain
ATX1-F05	ATGGCGTGTTTTTCTAACGAAACCCAGATCG	Forward primer PCR amplification of ATX1
ATX1-F05AX	ATGGCGTGTTTTTCTAACGAAACCCAGATCG	Forward PCR primer from the beginning of the ATX1 gene
ATX1-F06	GTTGTATTGGCAGCTACTTTGGACGAA	Forward primer from the beginning of the PWWP domain
ATX1-F07	AAAGAATGAGTCAACTTCAAAAGGG	Forward primer from the DAST domain
ATX1-F102	ATTGATGGGGTGAATAAAG	Forward primer from the beginning of the second PHD domain
ATX1-R02	TTATTCTGCGGTCCAGTC	Reverse primer from the end of the SET domain
ATX1-R04	AGAGCGGCCGCTTATTCCTGCATGCCCTC	Reverse primer from end of the PWWP domain, includes *Not*I site
ATX1-R05	CTAGCGGCCGCTTAGGAAACATGGGACGATGG	Reverse primer from end of the DAST domain, includes a *Not*I site
ATX1-R101	CTTCATAGCACCCCCTAC	Reverse primer from end of first PHD domain
ATX2-F201	ATCGATGGGGTTAAGAAA	Primers for testing ATX2 expression in RNAi-SET line 3 (see text)
ATX2-R202	GCGAGAAGCATGAATATTTG	Primers for testing ATX2 expression in RNAi-SET line 3 (see text)
CLF-Fwd	GAATTCCAACAAAGGGTTTTAC	Primers for testing CLF expression in RNAi-SET line 3 (see text)
CLF-Rev	CTCGAGCTAAGCAAGCTTCTTGGGTC	Primers for testing CLF expression in RNAi-SET line 3 (see text)
PDIST-NcoI-Rev	AGATCTACCATGGTGCAGACAAAAAATATATAAATC A	Reverse primer for PCR amplification of DIST control promoter
pDIST-PstI-Fwd	GTCGACCTGCAGCAGGTACCTTGTCATTGCAT	Forward primer for PCR amplification of DIST control promoter
pSET-NcoI-Rev	CCATGGATTCATCTGTGACACCTTGG	Reverse primer for PCR amplification of solo-SET promoter
pSET-PstI-Fwd	CTGCAGACAGGTATGCAGCTACTGCGTT	Forward primer for PCR amplification of solo-SET promoter
SET-ATG-Rev	GTTGCTTGGAGTATTCATCTGTGACACCTTGGATCCGT G	Reverse primer for pcr amplification from the beginning of the SET domain

Supplemental Figures

Ndamukong_SF_1

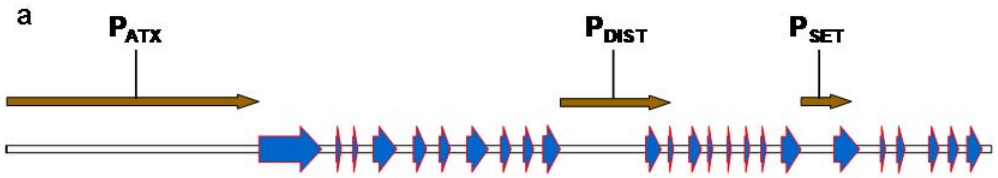

b

```
  1 acaggtatgc agctactgcg tttatctgtg gatgctaaga ttaaaattta gattcacacc acacttttgg gacaggatta tttcatcatt attcttttac
101 cttgcatacg gccatgtgtg ttttgttctc tttcatattc ttacatatcc tcttaagata tcagtttctt actttatata caagcatttt ttagatttga
201 tacaaaggtc aaatttcagg cttttgtgtt tccattcttt tctactttta ttcgtgtttg catcctatgg gtcagtatag atgataattt ccgtctattg
301 ttgcagagcc tTATAAttgt tttggcagaa gagggcgaaa ggaacctgaa gctcttgctg ctgcttcttc aaagcggtta tttgttgaga atcagccata
                                                                    M  N  T  P   S  N  I   L  S  M
401 tgttattggt ggttactcta gacttgagtt ttcaacgtac aaaagcattc acggatccaa ggtgtcacag ATGAATACTC CAAGCAACAT TCTTTCTATG
    A  E  K  Y   R  Y  M   R  E  T   Y  R  K  R   L  A  F
501 GCTGAGAAAT ATAGATACAT GAGGGAAACA TACAGGAAGA GATTAGCATT TGgtaagcat tcgttattct ttaactttca gtaaatctta aaagatatta
601 caggtctttt caacttctgc taagataaaa aatatagtag gatttctgta ggataaaaat aatttgtagg attcctttca gaatgatcta gtcacatcct
701 aagcttcttt cagaaaaatc ttataaaagt tggttctttt tttgtttcag
```

SF 1: Analysis of the putative promoter regions for *soloSET*

a) The regions of the ATX1 gene used as promoters for the *GUS* gene are indicated by arrows. P-ATX1 includes 2337 nt DNA sequence upstream of the first coding sequence; P-DIST is 1024 nt upstream of the SET domain containing a putative TATA-box; P-SET contains 476 nt immediately upstream of SET. Blue arrows are exons and black lines are intron sequences. Primes used for cloning are shown in Suppl. Table 1.

b) DNA sequences used to test promoter activity upstream of the SET domain. The sequences of the first SET domain exon are shown in red capital letters. Introns are lower case. The putative TATA-box is shown in bold caps and shadowed.

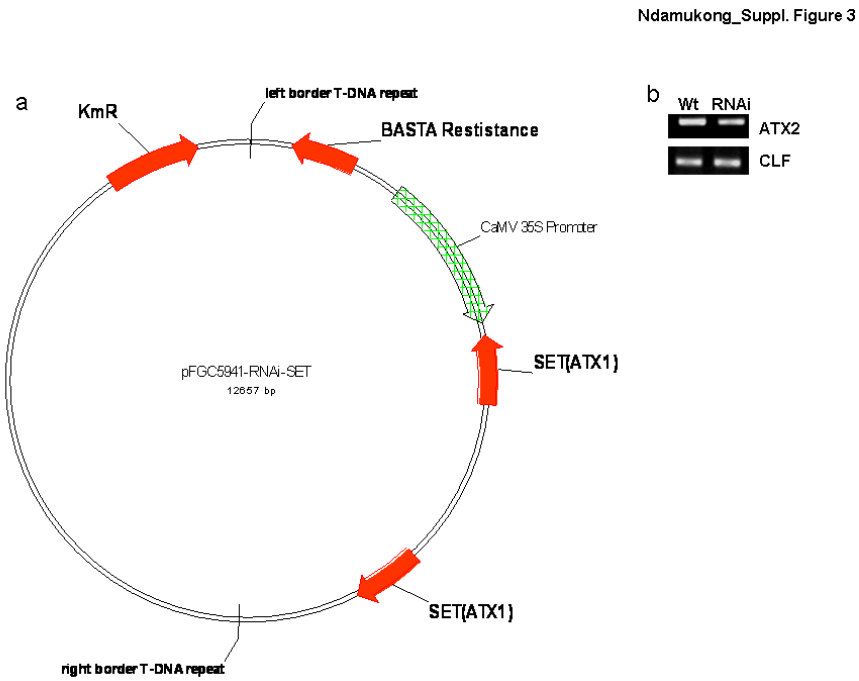

SF 2: The *RNAi-SET* construct used for the generation of stably expressing *Arabidopsis* lines

a) Structure of the destination vector pFGC5941. See Methods for details.

b) Transcripts from the *ATX2* and *CLF* genes detected in line 3 (from Figure 3a, text).
For *CLF* expression mRNA was isolated from flowers expressing *SET-RNAi*;

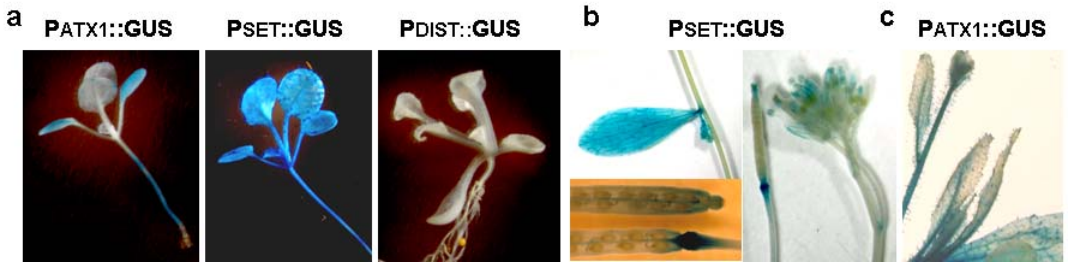

SF 3: Analysis of the putative promoter regions upstream of the SET domain

a) Transgenic seedlings stably expressing *GUS* fusion constructs under the promoter for the full-size ATX1 (P_{ATx1}::GUS), the 465 bp sequences 5'- of SET (P_{SET}::GUS), or a distally located region containing a putative TATA-box (P_{DIST}::GUS);

b) Mature transgenic plants expressing the P_{SET}::GUS construct. The strong staining in well-defined regions at organ attachment sites is notable.

c) Staining of mature transgenic plants expressing the P_{ATx1}::GUS construct is in the vascular tissues.

Ndamukong_SF 4a

```
   1 MACVSNETQI EIDVHDLVEA PIHYDSIESI YSIPSSALCC VNAVGSHSLM
  51 SKKVKAQKLP MIEQFEIEGS GVSASDDCCR SDDYKLRIQR PEIVRVYYRR
 101 RKRPLRECLL DQAVAVKTES VELDEIDCFE EKKRRKIGNC ELVKSGMESI
 151 GLRRCKENNA FSGNKQNGSS RRKGSSSKNQ DKATLASRSA KKWIRLSYDG
 201 VDPTSFIGLQ CKVFWPLDAL WYEGSIVGYS AERKRYTVKY RDGCDEDIVF
 251 DREMIKFLVS REEMELLHLK FCTSNVTVDG RDYDEMVVLA ATLDECQDFE
 301 PGDIVWAKLA GHSMWPAVIV DESIIGERKG LNNKVSGGGS LLVQFFGTHD
 351 FARIKVKQAI SFIKGLLSPS HLKCKQPRFE EGMQEAKMYL KAHRLPERMS
 401 QLQKGADSVD SDMANSTEEG NSGGDLLNDG EVWLRPTEHV DFRHIIGDLL
 451 IINLGKVVTD SQFFKDENHI WPEGYTAMRK FTSLTDHSAS ALYKMEVLRD
 501 AETKTHPLFI VTADSGEQFK GPTPSACWNK IYNRIKKVQN SDSPNILGEE
 551 LNGSGTDMFG LSNPEVIKLV QDLSKSRPSS HVSMCKNSLG RHQNQPTGYR
 601 PVRVDWKDLD KCNVCHMDEE YENNLFLQCD KCRMMVHAKC YGELEPCDGA
 651 LWLCNLCRPG APDMPPQCCL CPVVGGAMKP TTDGRWAHLA CAIWIPETCL
 701 SDVKKMEPID GVNKVSKDRW KLMCTICGVS YGACIQCSNN SCRVAYHPLC
 751 ARAAGLCVEL ENDMSVEGEE ADQCIRMLSF CKRHRQTSTA CLGSEDRIKS
 801 ATHKTSEYLP PPNPSGCART EPYNCFGRRG RKEPEALAAA SSKRLFVENQ
 851 PYVIGGYSRL EFSTYKSIHG SKVSQMNTPS NILSMAEKYR YMRETYRKRL
 901 AFGKSGIHGF GIFAKLPHRA GDMMIEYTGE LVRPSIADKR EQLIYNSMVG
 951 AGTYMFRIDD ERVIDATRTG SIAHLINHSC VPNCYSRVIT VNGDEHIIIF
1001 AKRHIPKWEE LTYDYRFFSI GERLSCSCGF PGCRGVVNDT EAEEQHAKIC
1051 VPRCDLIDWT AE
```

SF 4a: Coverage map of the ~120 kD 2D gel spot reacting with the antiATX1 antibody (see Figure 4a in text, arrowhead).
From MASCOT database search: Match to: gi|12659210 Score: 3083
Trithorax-like protein 1 [Arabidopsis thaliana];Matched peptides shown in bold red.
Score cut-off 35.

Ndamukong_SF 4b

```
 875 MNTPS NILSMAEKYR YMRETYRKRL
 901 AFGKSGIHGF GIFAKLPHRA GDMMIEYTGE LVRPSIADKR EQLIYNSMVG
 951 AGTYMFRIDD ERVIDATRTG SIAHLINHSC VPNCYSRVIT VNGDEHIIIF
1001 AKRHIPKWEE LTYDYRFFSI GERLSCSCGF PGCRGVVNDT EAEEQHAKIC
1051 VPRCDLIDWT AE
```

SF 4b: Coverage map of the ~22 kD spot from the 2D gel reacting with the ATX1 antibody (see Figure 4a in text, black arrow).
From MASCOT database search: Match to: gi|12659210 Score: 1083
Trithorax-like protein 1 [Arabidopsis thaliana]; Shown are sequencing corresponding to the soloSET. Matched peptides shown in bold red. Score cut-off 35.

Ndamukong_SF 5

```
  1 MGKEKFHINI VVIGHVGSGK STTTGHLIYK LGGIDKRVIE RFEKEAAEMN
 51 KRSFKYAWVL DKLKAERERG ITIDIALWKF ETTKYYCTVI DAPGHRDFIK
101 NMITGTSQAD CAVLIIDSTT GGFEAGISKD GQTREHALLA FTLGVKQMIC
151 CCNKMDATTP KYSKARYDEI IKEVSSYLKK VGYNPDKIPF VPISGFEGDN
201 MIERSTNLDW YKGPTLLEAL DQINEPKRPS DKPLRLPLQD VYKIGGIGTV
251 PVGRVETGMI KPGMVVTFAP TGLTTEVKSV EMHHESLLEA LPGDNVGFNV
301 KNVAVKDLKR GYVASNSKDD PAKGAANFTS QVIIMNHPGQ IGNGYAPVLD
351 CHTSHIAVKF SEILTKIDRR SGKEIEKEPK FLKNGDAGMV KMTPTKPMVV
401 ETFSEYPPLG RFAVRDMRQT VAVGVIKSVD KKDPTGAKVT KAAVKKGAK
```

SF 5: Coverage map of the 50 kD protein band reacting with the maize EF1A antibody.
The band indicated by arrow (Figure 5a) was identified as EF1A. From MASCOT database search: Match to: gi|18086389 Score: 805. Matched peptides are shown in bold red. Score cut-off 35.

Ndamukong_SF 6a

```
  1 MGKEKFHINI VVIGHVDSGK STTTGHLIYK LGGIDKRVIE RFEKEAAEMN
 51 KRSFKYAWVL DKLKAERERG ITIDIALWKF ETTKYYCTVI DAPGHRDFIK    K79 Trimethyl, K55 Dimethyl
101 NMITGTSQAD CAVLIIDSTT GGFEAGISKD GQTREHALLA FTLGVKQMIC
151 CCNNIDATTP KYSKARYDEI IKEVSSYLKK VGYNPDKIPF VPISGFEGDN    K187 Trimethyl
201 MIERSTNLDW YKGPTLLEAL DQINEPKRPS DKPLRLPLQD VYKIGGIGTV
251 PVGRVETGMI KPGMVVTFAP TGLTTEVKSV EMHHESLLEA LPGDNVGFNV
301 KNVAVKDLKR GYVASNSKDD PAKGAANFTS QVIIMNHPGQ IGNGYAPVLD    K306 Trimethyl
351 CHTSHIAVKF SEILTKIDRR SGKEIEKEPK FLKNGDAGMV KMTPTKPMVV    K 396 Trimethyl
401 ETFSEYPPLG RFAVRDMRQT VAVGVIKSVD KKDPTGAKVT KAAVKKGAK
```

SF 6a: Coverage map of the spot identified by arrow in Figure 5d, WT panel (main text).
From MASCOT database search: Match to: gi|18086389 Score: 732; Score cut-off 35.
Modified di- and tri-methylated Lysines are highlighted in blue; monomethylated K55 is in blue.

Ndamukong_SF 6b

```
  1 MGKEKFHINI VVIGHVGSGK STTTGHLIYK LGGIDKRVIE RFEKEAAEMN
 51 KRSFKYAWVL DKLKAERERG ITIDIALWKF ETTKYYCTVI DAPGHRDFIK    K79 Trimethyl, K55 Dimethyl
101 NMITGTSQAD CAVLIIDSTT GGFEAGISKD GQTREHALLA FTLGVKQMIC
151 CCNKMDATTP KYSKARYDEI IKEVSSYLKK VGYNPDKIPF VPISGFEGDN    K187  Trimethyl
201 MIERSTNLDW YKGPTLLEAL DQINEPKRPS DKPLRLPLQD VYKIGGIGTV
251 PVGRVETGMI KPGMVVTFAP TGLTTEVKSV EMHHESLLEA LPGDNVGFNV
301 KNVAVKDLKR GYVASNSKDD PAKGAANFTS QVIIMNHPGQ IGNGYAPVLD    K306  Trimethyl
351 CHTSHIAVKF SEILTKIDRR SGKEIEKEPK FLKNGDAGMV KMTPTKPMVV
401 ETFSEYPPLG RFAVRDMRQT VAVGVIKSVD KKDPTGAKVT KAAVKKGAK
```

SF 6b: Coverage map of the spot identified by arrow in Figure 5d, RNAi-panel.
From MASCOT database search: Match to: gi|110741201 Score: 573; Modified di- and tri-methylated Lysines are highlighted in blue; monomethylated K55 is in blue. Note absent signal for a tri-methylated K396, yellow highlight; Score cut-off 35.